Ecotoxicology and Environmental Safety 304 (2025) 119132

Contents lists available at ScienceDirect

Ecotoxicology and Environmental Safety

journal homepage: www.elsevier.com/locate/ecoenv

3.5GHz radiofrequency electromagnetic fields (RF-EMF) on metabolic disorders in *Drosophila melanogaster*

Yahong Wang [b], Ziyan Zhang [a,c,*], Lu Zhang [e], Yanyan Liao [a,c,*], Peng Cai [a,c,d,*]

[a] Key Laboratory of Urban Environment and Health, Institute of Urban Environment, Chinese Academy of Sciences, Xiamen 361021, China
[b] Institute of Light Resources and Environmental Sciences, Henan Academy of Sciences, Zhengzhou 450002, China
[c] Xiamen Key Laboratory of Physical Environment, Xiamen 361021
[d] Shanghai Institute of Nutrition and Health, Chinese Academy of Sciences, Shanghai 200031, China
[e] the State Key Laboratory of Multimodal Artificial Intelligence Systems, Institute of Automation, Chinese Academy of Sciences, Beijing 100190, China

ARTICLE INFO

Keywords:
Drosophila melanogaster
3.5 GHz RF-EMF
Metabolomics
Differential metabolites
Metabolic disorders

ABSTRACT

The widespread implementation of fifth-generation (5 G) technology has raised concerns regarding its impact on biosafety. This study aims to uncover metabolic alterations in *Drosophila melanogaster* in response to electromagnetic radiation through metabolomics under 3.5 GHz radiofrequency electromagnetic fields (RF-EMF) conditions. Newborn male flies were continuously exposed to 3.5 GHz RF-EMF at intensities of 0.1 W/m^2, 1 W/m^2, and 10 W/m^2 throughout their entire life cycle under 24-hour constant darkness. Metabolomic analysis was performed on Drosophila samples after long-term exposure. The results indicate that long-term exposure to RF-EMF leads to disruptions in four metabolic pathways - alanine, aspartate and glutamate metabolism, tryptophan metabolism, ascorbate and aldehyde metabolism, and purine metabolism - as well as 34 differential metabolites across various power density in *Drosophila melanogaster*. Notably, the most significant metabolites (GABA, glucose-6-phosphate, AMP, N-formylglycinamide nucleotide, LPC, and MG) exhibited high sensitivity to RF-EMF showing significant decreases. The suggests that long-term exposure to electromagnetic wave treatment may reduce the overall metabolic levels in fruit fly. These findings provide valuable insights into the metabolic disturbance induced by RF-EMF and enhance our understanding of the potential health effects associated with 5 G radiation.

1. Introduction

The emergence of the fifth generation (5 G) mobile communication technology has been driven by the exponential growth in human and societal demand for wireless communication. While the global deployment of 5 G frequency bands involves nonionizing radiation, concerns about its health and safety persist(Karipidis et al., 2021). In recent years, a large number of studies in safety assessment (Betta et al., 2023; Di Ciaula, 2018) and experimental research (Joushomme et al., 2023; Wang et al., 2022; Yang et al., 2022) have proposed that 5 G radiofrequency radiation will cause health problems and biological effects, whether positive or negative, there is a lot of controversy, and there is a lack of sufficient scientific basis. We hope that research on the health effects of 5 G will provide a strong scientific basis to avoid many unfounded assumptions.

In 2011, the International Agency for Research on Cancer (IARC) classified radiofrequency electromagnetic radiation (RF-EMF) as a possible carcinogen (IARC., 2013), although the evidence supporting this claim was weak and lacked scientific basis. The most recent RF exposure guidelines and standards, which also encompass the 5 G band, primarily aim to restrict RF-induced short-term heating and prevent tissue warming (Lin, 2023). Significant attention has been focused on the effects of RF radiation prior to the advent of 5 G. It has been suggested that RF radiation can induce the production of free radicals, leading to oxidative stress (Amiri et al., 2023; Nazıroğlu4, 2018), impact the neurological system(Cordelli et al., 2023; Mumtaz et al., 2022), result in cognitive dysfunction(Verbeek et al., 2021), cause sleep disorders(Deng et al., 2024; Eggert et al., 2020; Wang et al., 2021) and potentially contribute to carcinogenesis(Gökçek-Saraç et al., 2021; Gorski et al., 2021; Karipidis et al., 2025). Biological effects caused by

* Correspondence to: Institute of Urban Environment, Chinese Academy of Sciences, No. 1799, Jimei Avenue, Jimei District, Xiamen 361021, China.
E-mail addresses: zyzhang@iue.ac.cn (Z. Zhang), yyliao@iue.ac.cn (Y. Liao), pcai@sibs.ac.cn, pcai@iue.ac.cn (P. Cai).

https://doi.org/10.1016/j.ecoenv.2025.119132
Received 18 June 2025; Received in revised form 16 September 2025; Accepted 25 September 2025
Available online 6 October 2025
0147-6513/© 2025 The Authors. Published by Elsevier Inc. This is an open access article under the CC BY-NC-ND license (http://creativecommons.org/licenses/by-nc-nd/4.0/).

RF-EMF can be categorized into thermal and non-thermal effects. In general, the thermal effects are understood as the local temperature at the radiofrequency of the electric field through the oscillation current (Gye and Park, 2012; Jagbir Kaur, 2021), while non-thermal effects pertain to the energy absorbed by the tissue including the generation of large and damaging reaction oxygen species (ROS).

Numerous experimental studies have consistently demonstrated the ability of electromagnetic radiation to induce ROS formation (Bektas et al., 2022; Bouji et al., 2020; Choi et al., 2020; Kesari et al., 2011; Lai, 2019; Mortazavi and Mortazavi, 2016). Furthermore, studies have elucidated the existence of antioxidant defense mechanisms against electromagnetic field (EMF)-induced stress (Ehnert et al., 2017). However, comprehensive scientific evidence linking epidemiological associations and potential long-term negative health consequences is currently lacking. Several studies have proposed that increased transcription of oxidative stress genes in organisms can lead to alterations in cholesterol metabolism, resulting in a reduced growth rate (Piccinetti et al., 2018). Additionally, exposure to 1950 MHz radiofrequency radiation was found to significantly increase glucose metabolism in the hippocampus and amygdala regions of the brains of 5xFAD mice (Son et al., 2018). Furthermore, long-term exposure to microwave radiation may induce testicular damage by triggering oxidative stress through the disruption of hormonal balance and energy metabolism (Yao et al., 2025). In summary, the response of organisms to electromagnetic radiation encompasses not only oxidative stress but also metabolic changes. Unfortunately, although there are more research on the biological effects caused by microwave bands above 6 GHz in the 5 G bands (Karipidis et al., 2021), the scientific basis of the 3.5 GHz band below 6 GHz is only a few studies (Altman et al., 2016; Bektas et al., 2022; Joushomme et al., 2023; Wang et al., 2022, 2021; Yang et al., 2022; Zubair et al., 2020). It reveals the potential impact of several stress response routes.

Drosophila melanogaster was chosen as the experimental model due to its well-characterized genetics, short life cycle, and high reproductive rate, which allow for efficient multi-generational studies. Moreover, many of its cellular and molecular pathways, including those involved in oxidative stress, energy metabolism, and neurobiology, are highly conserved with mammals, making it a suitable organism for studying the biological effects of RF-EMF exposure. The availability of powerful genetic tools and metabolomic profiling techniques in Drosophila further facilitates the identification of biomarkers and mechanistic pathways underlying RF-EMF-induced biological responses.

This study aimed to examine the impact of long-term exposure to 3.5 GHz frequency, which simulates a mid-band RF radiation field similar to that of 5 G mobile communications, on *Drosophila melanogaster*. By analyzing the alterations in endogenous small molecule metabolites, we identified the metabolic processes and specific metabolites associated with the response to radiofrequency radiation. The objective of this research was to identify the differential metabolites that exhibit significant impacts in response to electromagnetic radiation, with the intention of providing valuable insights for further investigations into the targets of electromagnetic radiation.

2. Material and Methods

2.1. Fly lines and experimental conditions

The experimental model used in this study was the wild-type *Drosophila melanogaster* Canton S strain obtained from the Drosophila Resource and Technology Platform at the Institute of Biochemistry and Cellular Sciences, Shanghai Institutes for Biological Sciences, Chinese Academy of Sciences. The flies were cultured at 25 ± 0.5 ℃ and 60 % relative humidity (RH). Male flies from the F1 generation were selected for the experiment.

2.2. Long-term RF radiation exposure

The RF electromagnetic exposure system used in this study was shown in Fig. 1. For the evaluation of specific absorption rate (SAR) in our study, we adopted the same method (Supplementary 1) as the previous report (Wang et al., 2022). The SAR values corresponding to power density of 0.1 W/m^2, 1 W/m^2, and 10 W/m^2 were 0.0026 W/kg, 0.026 W/kg, and 0.26 W/kg.

For the long-term RF-EMF exposure, newborn female and male fruit flies were placed in the same tubes. Each group consisted of 10 parallel tubes exposed to RF-EMF at intensities of 0.1 W/m^2 (E0.1), 1 W/m^2 (E1), and 10 W/m^2 (E10). Sham-exposed (SE) flies were placed in Faraday shielded cages to maintain the same ambient temperature as the exposed groups. Parental flies were removed after three days of exposure. The developing F1 offspring remained in the RF-EMF environment throughout their larval and pupal stages until metamorphosis was completed.

2.3. Reactive oxygen species (ROS) detection

After exposure, male flies from the F1 generation were collected. The samples were centrifuged at low temperature with a force of 12,000 g for 10 min to obtain the supernatant. The supernatant was then stained with 1 μM DCFH-DA at 37℃ for 40 min, and fluorescence intensity was measured with excitation wavelengths set at 488 ± 10 nm and emission wavelengths at 525 ± 20 nm.

2.4. Enzyme activity assay

The supernatant from the F1 generation male flies was collected and analyzed for protein quantification (TP) (Komas Brilliant Blue method), total antioxidant capacity (T-AOC), superoxide dismutase (SOD) (WST-1), glutathione peroxide (GSH-PX) and catalase (CAT) (ammonium molybdate method) using assay kits. GSH-PX and CAT were analyzed separately according to the instructions.

2.5. Sample collection and preparation in metabolomics

F1 generation male flies were collected after long-term exposure and stored in the refrigerator. Metabolites were extracted using a methanol-water system. Flies were added to a real break tube with 1.0 mL of pre-cooled methanol/water (1:1, v/v) at −20°C. The tissue was then disrupted using a high-throughput tissue breaker (FastPrep-24, USA) at a frequency of 65 Hz for 120 s. Following the disruption, the tissue was centrifuged at 15,800 g for 15 min at 4°C. The resulting supernatant was carefully transferred to a centrifuge tube, while the tissue residue was discarded. The supernatant was concentrated to dryness using a vacuum centrifuge concentrator. The dried extract was then re-dissolved in 200 μL of methanol-water (1:1, v/v) and vortexed for 1–2 min until completely dissolved, then centrifuged at 15,800 g for 15 min at 4°C. The supernatant was removed from the liquid chromatography vial and prepared for detection. An equal amount from each Drosophila sample was mixed and prepared as a quality control (QC) sample to be tested on the machine.

2.6. Chromatographic and mass spectrometric conditions in metabolomics

The metabolomics chromatographic separation was performed using a reverse liquid phase separation system with a methanol-water system for the separation of *Drosophila metabolites*. A 10 μL injection volume was used, with the column temperature set at 50°C and the sample chamber temperature maintained at 4°C. The mobile phase A and B consisted of ultrapure water containing 0.1 % formic acid and methanol containing 0.1 % formic acid, respectively, with a flow rate of 0.4 mL/min. The elution gradient followed the following protocol: the initial mobile phase was 100 % A from 0 to 1.0 min, followed by a transition

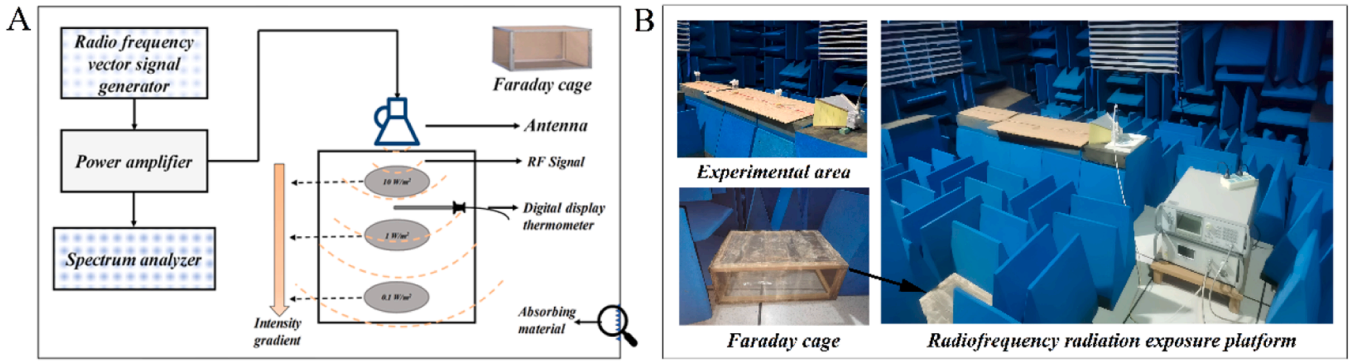


Fig. 1. RF-EMF exposure system. (A) Schematic diagram; (B) Photograph of the entire exposure setup. The signal from the vector signal source (Agilent Company 3, USA) is first amplified by the power amplifier (Qingdao Zhongdian Instrument Co., Ltd.) before being transmitted to the transmitting antenna (Qingdao Zhongdian Instrument Co., Ltd.), emitting an electromagnetic field. The specific power density employed in the experiment is monitored and analyzed by the electromagnetic radiation analyzer (PMM8053A, PMM).

from 100 % A to 95 % B from 1.0 to 21.0 min, then a transition from 95 % to 100 % B from 21.0 to 22.0 min, and finally a 100 % B mobile phase from 22.0 to 24.0 min. The Q-Exactive mass spectrometer uses an ESI source with a mass spectrometer scan range of 100–1000 Da and a full scan mode to collect data for both positive and negative ions simultaneously. Nitrogen was used as the carrier gas, and the injector voltage was 3.5 kV in both positive and negative ion modes. 50 L/min of sheath gas and 12.5 L/min of auxiliary gas were used. The capillary temperature was set at 350 °C.

2.7. Metabolomic data pre-processing

The raw data files obtained from UPLC-MS were processed using Compound Discoverer 2.1 (Thermo Fisher Scientific, USA; CD 2.1) software and further normalized using the 'stat The QC-RLSC method in the 'target' package of the R language platform. Principal component analysis (PCA) and Orthogonal Partial Least Squares Discriminant Analysis (OPLS-DA) were performed for data analysis using SIMCA-P software (Version 14.1, Umetrics, Umea, Sweden). Differential metabolites were selected based on Variable Importance for the Projection (VIP) score (≥1.5) and further confirmed using metabolite databases (HMDB, http://www.hmdb.ca) and comparison with MS spectra. Furthermore, a non-parametric test for metabolites between groups was performed using MetaboAnalyst 5.0 (http://www.metaboanalyst.ca/), and the P-values were corrected (adjusted-P < 0.05) to establish statistical significance. Metabolites were considered sensitive to RF-EMF exposure if they exhibited a fold change in mean (FC) greater than 2.0. The final identification of significant differential metabolite molecules with altered metabolic profiles due to RF-EMF exposure was based on a combination of VIP, FC, and adjusted-P values.

2.8. Key differential metabolites detection

Male F1 flies exposed to long-term exposure were collected, and the samples were homogenized using a high-throughput tissue homogenizer (SCIENTZ-192, Shanghai Wanbo Biotechnology Co., Ltd.). After homogenization, the samples were centrifuged at 5000 g for 10 min at low temperature, and the supernatant was collected. The supernatant was then analyzed for key differential metabolites or related enzyme activity levels, including adenosine monophosphate (AMP), peptidoglycan (PG), monoacylglycerol lipase (MAGL), phospholipase A2 (PLA2), and glycinamide ribonucleotide transformylase (GART), using an ELISA kit. The kit employs a double-antibody sandwich ELISA technique. The absorbance (OD value) was measured at a wavelength of 450 nm using a microplate reader, and the sample concentrations were calculated according to the instructions provided by the ELISA kit.

2.9. Statistical analysis

The experimental data were processed using IBM SPSS 20 Statistics software and Microsoft Excel. One-way Analysis of Variance (ANOVA) method and Least Significant Difference (LSD) method were used to analyze the means and test the significance of differences. A significance level of $P < 0.05$ was considered statistically significant (*, $P < 0.05$; **, $P < 0.01$). The experiment was all repeated three times.

3. Results

3.1. Screening for differential metabolites in F1 male

Data from different exposure power density conditions were initially tested and visualized using the OPLS-DA model. The results of the 999permutation test confirmed the reliability of the model (Fig. 2ABCD). The OPLS-DA model showed that the distance between sample points reflected the strength of correlation. Although there were inter-individual differences among the different power density conditions, the exposed and sham-exposed samples were clearly distinguishable, exhibiting significant clustering on the first principal component (PC1) (Positive model: R2X = 0.585, R2Y = 0.975, Q2 = 0.577; Negative model: R2X = 0.641, R2Y = 0.973, Q2 = 0.704). From the positive and negative models, a total of 98 and 45 common differential metabolites, respectively, were identified among all exposed and sham-exposed samples. These findings suggest that RF-EMF leads to discernible variations in the principal component analysis of metabolites in male flies.

The obtained HMDB IDs from the HMDB platform were used to validate the identification of the 143 differential metabolites. The important HMDB ID numbers of the differential metabolites were then input into the Pathway Analysis module of MetaboAnalyst 5.0 to explore the enrichment of these endogenous differential metabolites in fruit flies. The results revealed that long-term exposure to 3.5 GHz RF-EMF disturbed 14 metabolic pathways in F1 male flies. Notably, the pathways affected to a greater extent included alanine aspartate and glutamate metabolism, tryptophan metabolism, ascorbate and aldarate metabolism, and purine metabolism (Fig. 2E, Supplementary Table 1). Therefore, long-term 3.5 GHz RF-EMF may mainly affect 4 metabolic pathways in male flies.

3.2. Changes in differential metabolites in F1 generation male

The OPLS-DA model was utilized to identify differential metabolites with VIP values greater than 1.5, and the variation in these metabolites was visualized through clustering analysis using RStudio software. The overall trend of all differential metabolites in the E0.1, E1, E10, and C

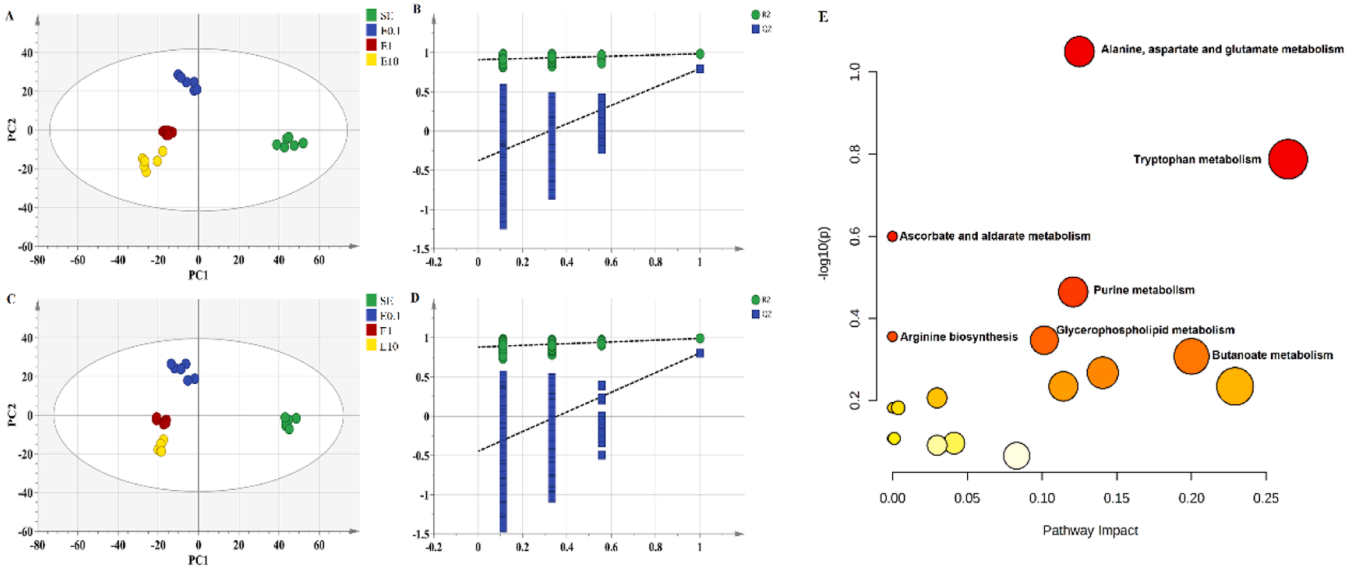


Fig. 2. The long-term exposure to RF-EMF on OPLS-DA model analysis of F1 male. (A) Score diagram of Positive OPLS-DA analysis. (B) 999 replacement tests of Positive OPLS-DA model. (C) Score diagram of Negative OPLS-DA analysis. (D) 999 replacement tests of Negative OPLS-DA model. (E) Metabolic pathway enrichment results.

groups is depicted in the heatmap (Fig. 3D), where the gradient change in color intensity represents the similarity of differential metabolites among these groups. The clustering tree illustrates the similarity between groups and differentiates among various differential metabolites.

To further analyze the differences in the effects on differential metabolites at different exposure power densities, volcano plots were employed. Metabolites were considered significantly up-regulated if the fold change was more than 2-fold, significantly down-regulated if it was less than 0.5, and $P < 0.05$ was set as the screening criterion. In Fig. 3, the results revealed that under E0.1 conditions, 57 metabolites exhibited significant differences compared to the sham-exposed samples (up-regulated: 12, down-regulated: 45); similarly, under E1 conditions, 59 metabolites showed significant differences (up-regulated: 14, down-regulated: 45); and under E10 conditions, 73 metabolites demonstrated significant differences (up-regulated: 19, down-regulated: 54). Based on these findings, we further refined the list of differential metabolites for each exposure intensity, ranking them according to the VIP value (>1.5) from highest to lowest. Consequently, we identified 34 co-important differential metabolites affected by different intensities of RF-EMF (Table 1). For specific descriptive information, please refer to Table 1. Therefore, after long-term 3.5 GHz RF-EMF, we successfully identified 34 significant differential metabolites in male flies, demonstrating their distinct response to radiofrequency radiation at different intensities.

3.3. Potential interactions between important differential metabolites

In order to further investigate the network interactions among the important differential metabolites in flies that respond sensitively to RF-EMF, the Spearman correlation of the aforementioned 34 commonly important differential metabolites was calculated using RStudio software. Fig. 4A illustrates the correlations among different important differential metabolites, with most of them showing positive correlations and a few displaying negative correlations. In the network interaction analysis of the important differential metabolites (Fig. 4B), 13 strongly correlated metabolites were identified. These included organic compounds such as 1-(1,2,3,4,5-pentahydroxypent-1-yl)-1,2,3,4-tetrahydro-beta-carboline 3-carboxylate, TMTT (4,8,12-trimethyl-1,3,7,11-tridecatetraene), Tetrahydrodeoxycortisol, Tryptophylhydroxyproline, fatty alcohol compound (1-Acetoxy-2-hydroxy-16-heptadecyn-4-one, 4′-o-methyl-(-)-epicatechin-3′-o-beta-Glucuronide), fatty acyl glycosides (Dihydrozeatin-9-N-glucoside-O-glucoside), 3-methoxy-chromone compounds (3-Methoxy-2-(4-methylbenzoyl)-4h-1-benzopran-4-one), Orotidine, LysoPE(0:0/20:0), LysoPE(0:0/16:0), LysoPC(18:3(6Z,9Z,12Z)/0:0), and AMP (Adenosine monophosphate). Furthermore, in Fig. 5B, the red dots represent differential metabolites with strong correlations, and the size of the dots within the module indicates the strength of the correlation. Larger dots indicate stronger correlations, while the green dots distributed in the periphery are relatively smaller, indicating weaker correlations with other metabolites. Hence, the results reveal a predominantly positive correlation among the 34 significant differential metabolites in male flies, with 13 of them exhibiting a particularly robust correlation under long-term radiofrequency radiation.

3.4. Key differential metabolites response to RF-EMF

In our study, we identified 34 common important differential metabolites that are involved in processes such as alanine, aspartate, and glutamate metabolism, purine metabolism, and lipid metabolism. Among these metabolic processes, the key differential metabolites are primarily GABA, glucose-6-phosphate, AMP, N-formylglycinamide nucleotide, LPC, and MG. These six metabolites showed higher sensitivity to RF-EMF exposure. Further analysis of the structures and specific changes of these metabolites in response to different intensities of RF-EMF exposure (Fig. 4CDEFGH) revealed significant reductions in GABA, glucose-6-phosphate, AMP, N-formylglycinamide nucleotide, LPC, and MG in Drosophila. Therefore, these findings suggest that these metabolites may play a crucial role in the response to RF-EMF exposure.

3.5. The quantitative validation of key differential metabolites in the F1 male flies

In the metabolomic analysis, we successfully detected six key differential metabolites. To further explore the specificity and sensitivity of these metabolites to radiofrequency radiation, we conducted additional validation of the levels of these metabolites or their related enzyme activities. The changes in GABA levels have been reported in our previous studies, indicating that electromagnetic radiation can significantly reduce its concentration (Wang et al., 2021). Fig. 5 shows the changes in the levels of the other five small molecules detected by the ELISA kit

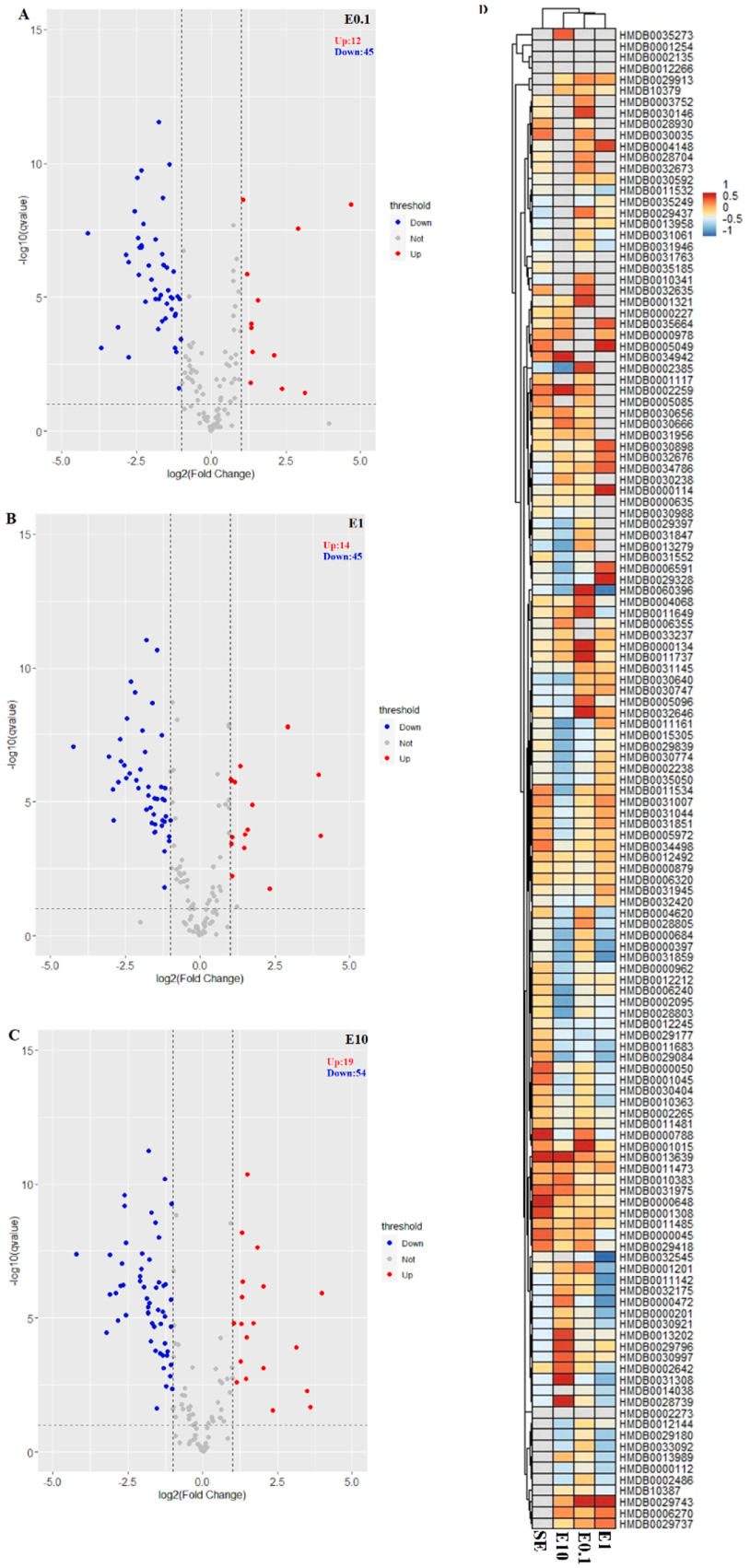


Fig. 3. Volcanic map of significantly metabolic in F1 male. (A) E0.1 vs SE; **(B)** E1 vs SE**; (C)** E10 vs SE. (D) Heat map of significantly metabolic in F1 male.

Table 1
Metabolites sensitive to 3.5 GHz RF-EMF in F1 male.

Compound	Name	Formula	VIP	FC			Adjusted P value		
			E0.1, E1, E10 vs SE	E0.1 vs. SE	E1 vs. SE	E10 vs. SE	E0.1 vs. SE	E1 vs. SE	E10 vs. SE
HMDB0029913	Gynocardin	$C_{12}H_{17}NO_8$	4.59	0.31	0.24	0.28	0.0000	0.0000	0.0000
HMDB0001254	Glucosa mine 6-phosphate	$C_6H_{14}NO_8P$	4.55	0.45	0.40	0.34	0.0000	0.0000	0.0000
HMDB10387	LysoPC(18:3(6Z,9Z,12Z)/0:0)	$C_{26}H_{48}NO_7P$	4.54	0.32	0.35	0.39	0.0001	0.0001	0.0003
HMDB0035273	1-Acetoxy−2-hydroxy−5,12,15-heneicosatrien−4-one	$C_{23}H_{38}O_4$	4.04	0.06	0.05	0.05	0.0000	0.0000	0.0000
HMDB0000112	Choline	$C_4H_9NO_2$	3.49	0.30	0.32	0.31	0.0000	0.0000	0.0000
HMDB0013989	O-Desmethylnaproxen	$C_{13}H_{12}O_3$	3.47	0.27	0.30	0.28	0.0000	0.0000	0.0000
HMDB0029180	4'-O-methyl-(-)-epicatechin−3′-O-beta-glucuronide	$C_{23}H_{26}O_{12}$	3.26	0.11	0.13	0.11	0.0001	0.0000	0.0000
HMDB0029743	9H-Carbazole−3-carboxaldehyde	$C_{13}H_9NO$	3.22	0.44	0.44	0.37	0.0011	0.0007	0.0002
HMDB0000788	Orotidine	$C_{10}H_{12}N_2O_8$	3.17	0.27	0.18	0.13	0.0000	0.0000	0.0000
HMDB0002486	Taurochenodeoxycholate−3-sulfate	$C_{26}H_{45}NO_9S_2$	3.12	0.44	0.35	0.29	0.0000	0.0000	0.0000
HMDB0012144	2-A mino−4-oxo−6-(1′,2′,3′-trihydroxypropyl)-diquinoid−7,8-dihydroxypterin	$C_9H_{15}N_5O_6$	2.98	8.71	16.30	11.17	0.0364	0.0002	0.0051
HMDB0006270	Linoelaidic acid	$C_{18}H_{32}O_2$	2.96	0.40	0.44	0.38	0.0000	0.0001	0.0000
HMDB0033092	3-(1-Hydroxymethyl−1-propenyl)pentanedioic acid	$C_9H_{14}O_5$	2.92	0.37	0.25	0.26	0.0000	0.0000	0.0000
HMDB0029084	Tryptophylhydroxyproline	$C_{16}H_{19}N_3O_4$	2.48	0.18	0.22	0.17	0.0000	0.0000	0.0000
HMDB0034498	(3*E*,7*E*)−4,8,12-Trimethyl−1,3,7,11-tridecatetraene	$C_{16}H_{26}$	2.47	0.14	0.15	0.15	0.0000	0.0000	0.0000
HMDB0002095	Malonylcarnitine	$C_{10}H_{17}NO_6$	2.46	15.32	209.01	55.13	0.5424	0.0000	0.0194
HMDB0001308	5'-Phosphoribosyl-N-formylglycinamide	$C_8H_{15}N_2O_9P$	2.42	0.33	0.33	0.30	0.0000	0.0000	0.0000
HMDB0002385	Celastrol	$C_{29}H_{38}O_4$	2.41	5.19	4.97	5.12	0.0260	0.0180	0.0279
HMDB0031007	1-Acetoxy−2-hydroxy−16-heptadecyn−4-one	$C_{19}H_{32}O_4$	2.32	0.19	0.13	0.12	0.0000	0.0000	0.0000
HMDB0013639	8-[(A minomethyl)sulfanyl]−6-sulfanyloctanoic acid	$C_9H_{19}NO_2S_2$	2.31	0.21	0.18	0.29	0.0000	0.0000	0.0000
HMDB0011534	MG(0:0/16:1(9Z)/0:0)	$C_{19}H_{36}O_4$	2.17	0.20	0.12	0.12	0.0000	0.0000	0.0000
HMDB0005972	Tetrahydrodeoxycortisol	$C_{21}H_{34}O_4$	2.10	0.18	0.16	0.15	0.0000	0.0000	0.0000
HMDB0000045	Adenosine monophosphate	$C_{10}H_{14}N_5O_7P$	2.05	0.39	0.30	0.28	0.0000	0.0000	0.0000
HMDB0031975	3-Methoxy−2-(4-methylbenzoyl)−4H−1-benzopyran−4-one	$C_{18}H_{14}O_4$	1.97	0.25	0.23	0.28	0.0000	0.0000	0.0000
HMDB0031044	Avocadene 2-acetate	$C_{19}H_{36}O_4$	1.91	0.19	0.20	0.23	0.0000	0.0000	0.0000
HMDB0031851	3-(5,6,6-Trimethylbicyclo[2.2.1]hept−1-yl) cyclohexanol	$C_{16}H_{28}O$	1.83	0.20	0.17	0.23	0.0000	0.0000	0.0000
HMDB0011683	Molybdopterin precursor Z	$C_{10}H_{12}N_5O_7P$	1.82	0.20	0.20	0.33	0.0000	0.0000	0.0000
HMDB0012492	1-(1,2,3,4,5-Pentahydroxypent−1-yl)−1,2,3,4-tetrahydro-beta-carboline−3-carboxylate	$C_{17}H_{22}N_2O_7$	1.81	0.30	0.37	0.42	0.0000	0.0000	0.0000
HMDB0011473	LysoPE(0:0/16:0)	$C_{21}H_{44}NO_7P$	1.77	0.34	0.35	0.44	0.0001	0.0001	0.0002
HMDB0030146	(3xi,6E)−1,7-Diphenyl−6-hepten−3-ol	$C_{19}H_{22}O$	1.74	2.32	2.53	2.54	0.0000	0.0000	0.0000
HMDB0011481	LysoPE(0:0/20:0)	$C_{25}H_{52}NO_7P$	1.68	0.38	0.29	0.29	0.0000	0.0000	0.0000
HMDB0028803	Gluta minylmethionine	$C_{10}H_{19}N_3O_4S$	1.63	0.15	0.37	0.16	0.0000	0.0000	0.0000
HMDB0033237	1,2,10-Trihydroxydihydro-trans-linalyl oxide 7-O-beta-D-glucopyranoside	$C_{16}H_{30}O_{10}$	1.62	25.73	15.56	15.81	0.0000	0.0000	0.0000
HMDB0012212	Dihydrozeatin−9-N-glucoside-O-glucoside	$C_{22}H_{35}N_5O_{11}$	1.58	0.27	0.16	0.17	0.0000	0.0000	0.0000

method in the exposed and the sham-exposed samples, as well as the corresponding p-values. Among them, the concentration of PLA2 significantly decreased in the exposed group ($p < 0.05$), meanwhile PG shows slight decreased at the intensity of 1 W/m^2 ($p < 0.05$). In Fig. 5F, we present the relationships between these key small molecule metabolites through a metabolic pathway diagram. Overall, the validation experiments show that most differential metabolites exhibited significant differences between the exposed and sham-exposed samples, which is consistent with the results from the metabolomic analysis.

3.6. Long-term RF-EMF on oxidative stress in the F1 male flies

Long-term exposure to radiofrequency radiation may affect the oxidative stress system in Drosophila, so the levels of ROS, T-AOC, MDA, SOD activity, CAT activity and GSH-PX activity were measured in flies. The results demonstrated (Fig. 6) that ROS levels were significantly lower in the E0.1, E1 and E10 groups compared to the sham-exposed group ($p < 0.01$). T-AOC and MDA levels did not show significant changes. However, SOD activity was significantly increased only in the E10 group ($p < 0.01$), while CAT activity was significantly lower in the E0.1, E1 and E10 groups ($p < 0.01$). Additionally, GSH-PX activity was significant increased only in the E10 group ($p < 0.01$). These findings suggest that long-term radiofrequency radiation affects ROS levels and anti-oxidative stress system in male flies.

4. Discussion and Conclusions

With the rapid global development of 5 G technology, concerns regarding the potential health effects of 5 G RF radiation have gained significant attention. However, there is a notable lack of studies investigating the biological effects of 5 G RF radiation, and the underlying mechanisms remain largely unknown. Therefore, in this study, we focused on exploring the impacts of RF radiation within the 3.5 GHz frequency band, which is a primary frequency range used in 5 G networks in China. Our study was to investigate the metabolic alterations of *Drosophila melanogaster* response to RF radiation, building upon the existing knowledge base established by previous studies (Wang et al., 2022).

To investigate the underlying mechanism of RF-EMF on growth, development and behavior effects, we investigated the metabolic response of *Drosophila melanogaster* to long-term exposure to 3.5 GHz RF-EMF and identified significant disruptions in multiple metabolic pathways. Through untargeted metabolomic analysis, we screened a total of 143 differentially expressed endogenous metabolites. These difference metabolites are intricately linked to four major metabolic pathways disrupted by RF-EMF exposure: (1) alanine, aspartate and glutamate metabolism, (2) tryptophan metabolism, (3) ascorbate and aldehyde metabolism, and (4) purine metabolism. Each of these pathways plays a crucial role in maintaining cellular and organismal homeostasis.

Observing the changes in metabolites between the exposed and

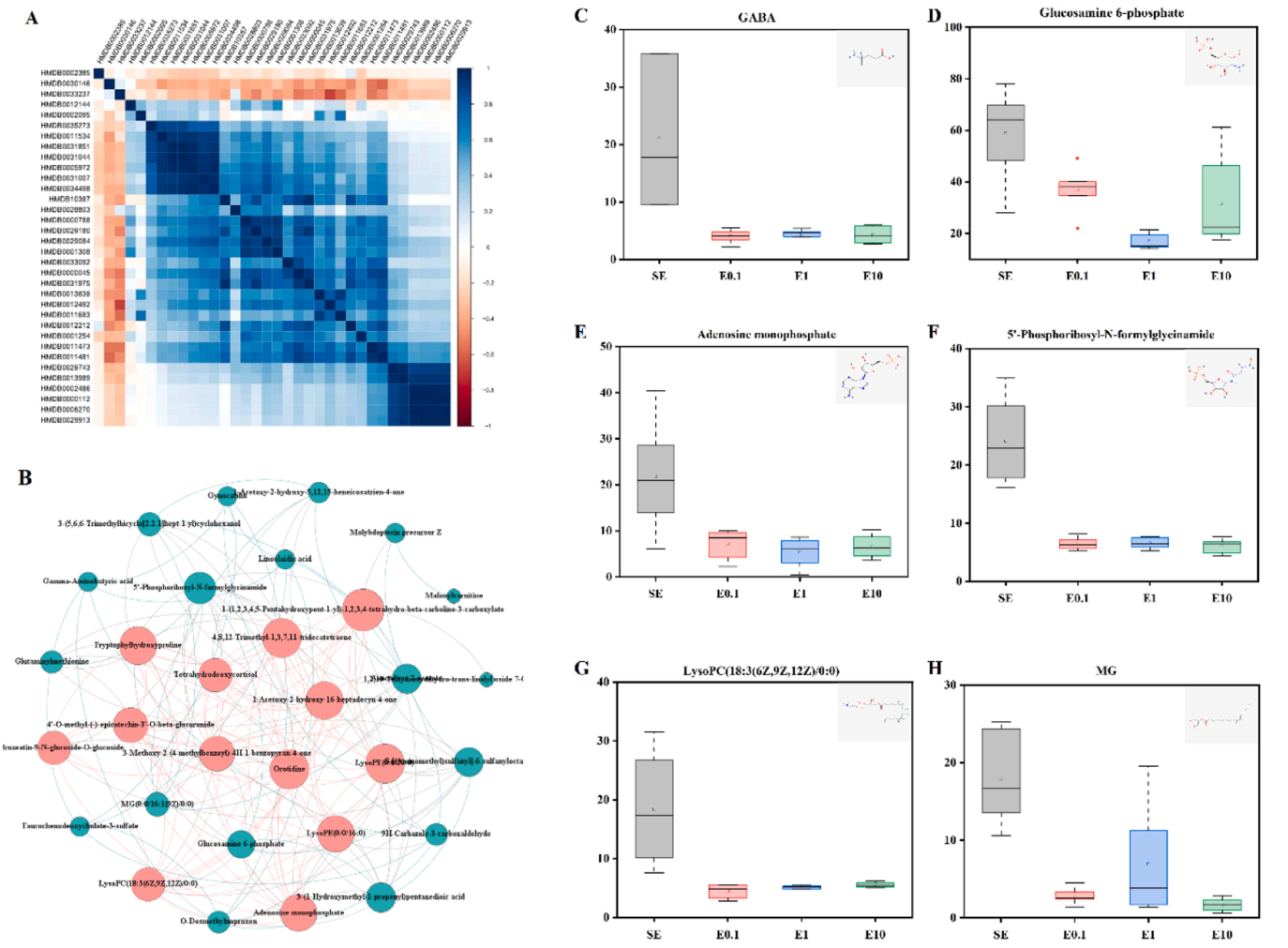


Fig. 4. Correlation analysis of important differential metabolites in F1 male. (A) Spearman correlation clustering analysis of important differential metabolites; (B) Network interactions among important differential metabolites ("Green" means weak interaction, "Red" means strong interaction). (C-H) Key differential metabolites in F1 male.

sham-exposed samples suggests that metabolic disturbances may accompany the organism's growth, development, and behavior. We identified 57, 59, and 73 differential metabolites under three different RF radiation exposure intensities. After excluding the effects of varying exposure doses on endogenous small molecule metabolites in Drosophila, we identified 34 commonly important differential metabolites that exhibited co-variance and held potential as biomarkers across the three exposure intensities. Glutamine, the most abundant amino acid in animals, plays crucial roles in antioxidant defense systems, biosynthesis, signal transduction, and energy metabolism in organisms (Altman et al., 2016). Additionally, elevated glutamine consumption is a common metabolic characteristic of cancer cells (Márquez et al., 2017) and is associated with their growth promotion (Kim, 2014). As glutamine is a precursor to glutathione, decreased levels of glutamine may indicate increased oxidative stress. Within the alanine, aspartate, and glutamate metabolic cycle, glutamate acts as an excitatory neurotransmitter involved in the regulation of the excitatory neurotransmitter system and is responsible for maintaining cognitive function and neuronal plasticity (Ding et al., 2021). In our study, we observed a reduction in glutamate-like GABA within the exposed group, specifically in the alanine, aspartate, and glutamate metabolic pathways. This aligns with the findings regarding GABA content in our previous research (Wang et al., 2021), suggesting that RF-EMF might impair the regulation of the neurotransmitter-mediated nervous system. Metabolites related to tryptophan metabolism can influence the synthesis of crucial neurotransmitters and hormones such as dopamine, epinephrine, and norepinephrine (Neurauter et al., 2008). Disruption in the synthesis process of these metabolites can have a significant impact on the nervous system (Wu et al., 2018). The effect of RF-EMF on the Drosophila nervous system may be a key factor influencing behavior.

Additionally, both growth and activity in Drosophila require the consumption of large amounts of ATP, which is broken down to produce ADP, which is hydrolyzed to AMP by kinase, which in turn produces IMP, which can be broken down to xanthine by hypoxanthine nucleotide dehydrogenase and can also resynthesize AMP (Chen et al., 2021). In our study, RF-EMF affects the purine metabolic pathway, with AMP and N-formylglycinamide nucleotide as its associated metabolites. AMP serves not only as a product of purine nucleotide synthesis but also of their oxidative catabolism. It can undergo oxidative phosphorylation to produce ATP, which provides a high-energy phosphate group. In our study, we also observed a relative reduction in AMP and N-formylglycinamide nucleotide levels. Our hypothesis suggests that RF-EMF intervention may promote purine nucleotide cycling. The significant effects of long-term RF-EMF on 34 important differential metabolites indicate its potential to modulate the body's immunity, antioxidant stress system, growth hormone, energy metabolism, and neurotransmitter system in response to environmental stressors affecting Drosophila. We also provide information on oxidative stress in fruit fly (Fig. 6).

Furthermore, several of the 34 important differential metabolites

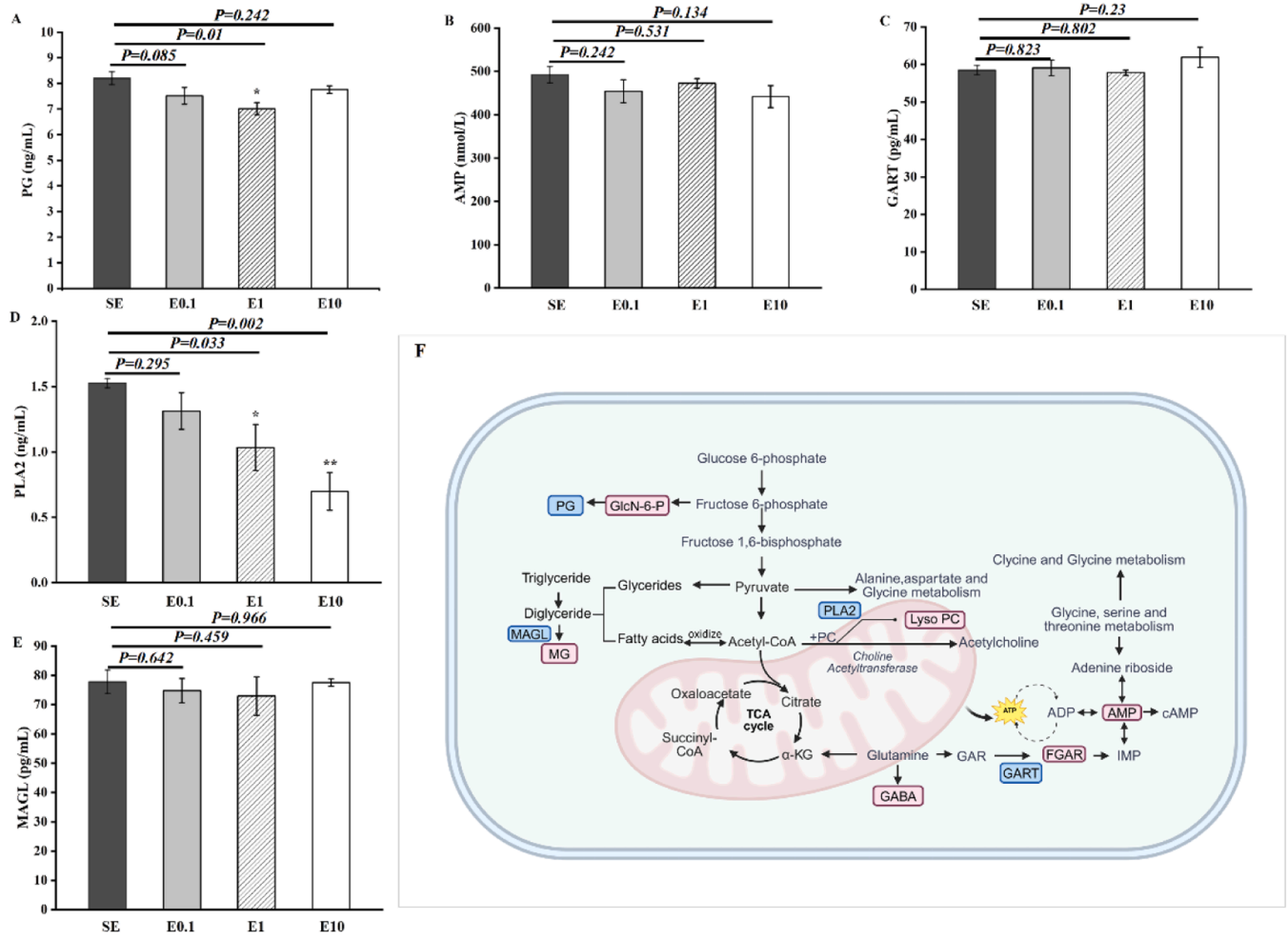


Fig. 5. Validation analysis of important differential metabolites in F1 male. (A) The content of PG; (B) The content of AMP; (C) The content of GART; (D) The content of PLA2; (E) The content of MAGL; (F) Important differential metabolites are involved in process in metabolic pathways. Red represents important differential metabolites screened in metabolomics, and blue represents small molecules detected in validation experiments. Values represent mean ± SEM. (*, $0.01 < p < 0.05$; **, $p < 0.01$).

identified are implicated in lipid metabolism, including LPC, LPE, MG, and glycerolipids, among others. The significant reductions in LPC and LPE, along with the notable increases in MG, suggest a dysregulation of lipid metabolism, particularly in lysophospholipids. Accumulation of lysophospholipids has been associated with cellular toxicity, and LPC (16:0)/(18:0) has been linked to brain inflammation (Bredehöft et al., 2019). Moreover, alterations in phospholipids, such as PC, LPC, and LPE, which consist of monounsaturated and polyunsaturated fatty acids, have been implicated in maintaining phospholipid homeostasis and are associated with neurodegenerative cognitive dysfunction. Although the frequency and intensity of radiofrequency radiation in our study were not expected to have a severe impact on cells or tissues, the significant reductions in LPC and LPE may be related to neurological modulation. MG, a minor component in most animal tissues, can disrupt cell membranes and typically does not accumulate under normal conditions. However, our study revealed a significant increase in MG levels, leading us to hypothesize that long-term RF radiation might cause damage to cell membranes. In summary, the six key differential metabolites most sensitive to the long-term RF-EMF response in our study were GABA, glucose-6-phosphate, AMP, N-formylglycinamide nucleotide, LPC, and MG.

For instance, GABA, a critical inhibitory neurotransmitter derived from glutamate, was significantly downregulated, suggesting a potential perturbation in neuronal signaling and amino acid turnover. Similarly, glucose-6-phosphate, a central intermediate of both glycolysis and the pentose phosphate pathway, showed marked reduction, implying compromised cellular energy production and redox balance. Two purine-related metabolites, AMP and N-formylglycinamide nucleotide, also declined significantly, pointing to possible interference with nucleotide biosynthesis and energy metabolism. These findings suggest that RF-EMF exposure may suppress the purine cycle and thereby impact DNA/RNA synthesis and ATP generation. Furthermore, LPC (lysophosphatidylcholine), a membrane lipid involved in inflammatory signaling, was decreased, which could indicate altered membrane dynamics or suppressed phospholipid turnover. Lastly, MG (putatively methylglyoxal or monoglyceride) reduction may reflect oxidative stress or impaired lipid catabolism.

We further verified the relationships of the six key differential metabolites in metabolic pathways by enzyme-linked immunosorbent assay. Previous studies have reported that electromagnetic radiation significantly decreases the levels of GABA in glutamate metabolic pathways(Wang et al., 2021), which is consistent with our findings. In our study, we also found a decreasing trend of PG in the glycolysis pathway under the density of 0.1 W/m^2, 1 W/m^2, and 10 W/m^2. This decrease may be triggered by the downregulation of the upstream metabolite GlcN-6-P, especially notable at 1 W/m^2, aligning with our earlier suggestion of a potential window effect at this exposure level. In the purine metabolic pathway, we observed a significant downward trend in AMP levels after exposure to electromagnetic radiation. Although the impact on GART was not as pronounced, it may be due to

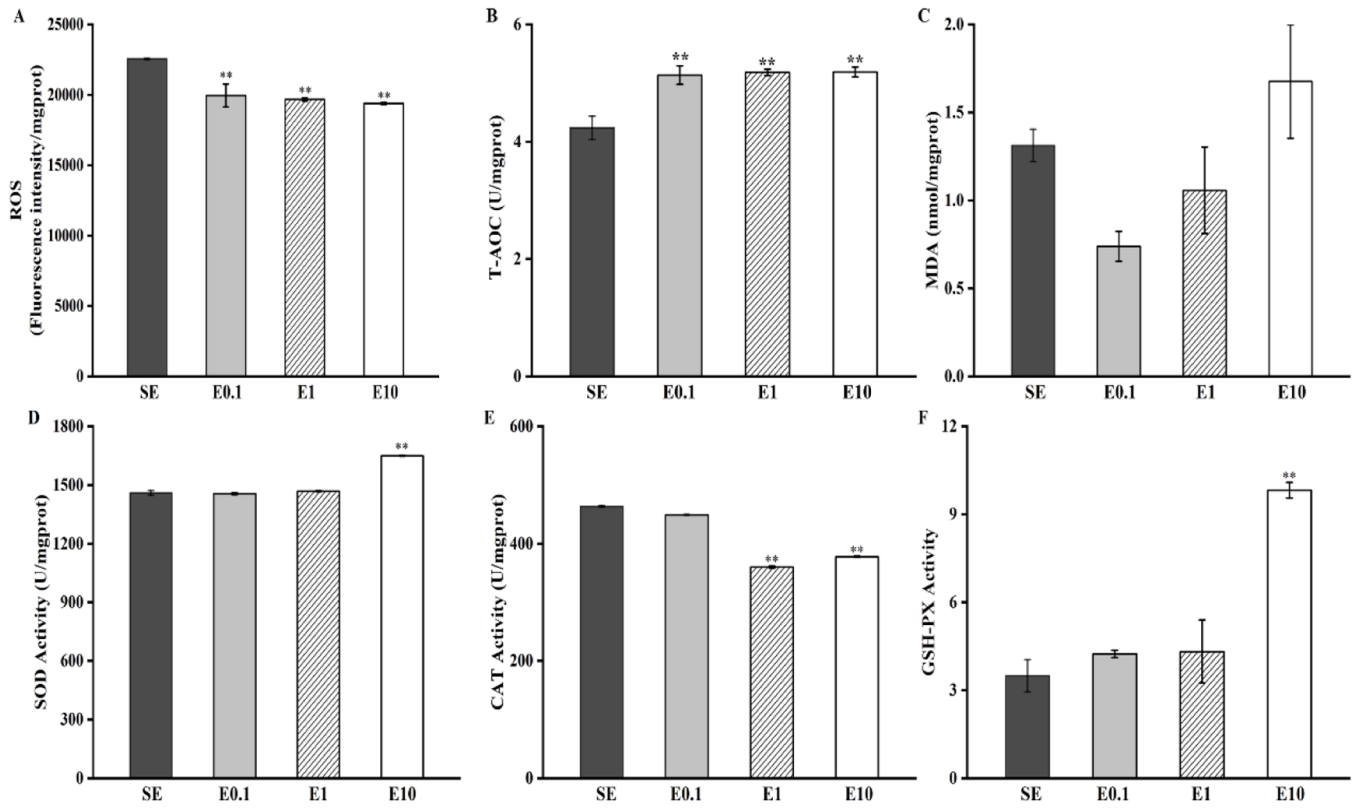


Fig. 6. The effects of long-term exposure to 3.5 GHz RF-EMF at different power density (0.1 W/m^2, 1 W/m^2 and 10 W/m^2) on oxidative stress in flies. The measurements were analyzed: ROS levels (A), total antioxidant capacity (T-AOC) (B), MDA (C), SOD enzyme activity (D), CAT enzyme activity (E), GSH-PX enzyme activity (F). Values represent mean ± SEM. (*, 0.01 <p < 0.05; **, p < 0.01).

enhanced downstream metabolism of FGAR, leading to a decrease in FGAR levels following electromagnetic exposure. During lipid metabolism, we found that the overall level of MAGL was not significantly affected by electromagnetic radiation, possibly due to a decrease in the upstream metabolites Diglyceride and Triglyceride, resulting in an overall declining trend of MG in the metabolic pathway. Additionally, PLA2 showed a significant decreasing trend under conditions of 0.1 W/m^2, 1 W/m^2, and 10 W/m^2, with a dependence on exposure intensity (Fig. 5D), leading to a decrease in downstream Lyso PC levels. Therefore, long-term exposure to 3.5 GHz electromagnetic radiation can disrupt energy metabolism, lipid metabolism, neurotransmitter metabolism, as well as glycine, serine, and threonine metabolism pathways in fruit flies.

In summary, our results demonstrate that long-term RF-EMF exposure induces systemic metabolic disturbances in Drosophila, affecting both energy metabolism and regulatory pathways linked to stress responses and neurotransmission. The most crucial differential metabolites—GABA, glucose-6-phosphate, AMP, N-formylglycinamide nucleotide, LPC, and MG—showed high sensitivity to RF-EMF showed significant decrease, indicating that long-term electromagnetic wave treatment may reduce the overall metabolic level in fruit fly. The observed pattern of downregulated metabolites suggests a global metabolic suppression, potentially as a protective or compensatory adaptation to chronic electromagnetic stress. These findings underscore the value of metabolomics in uncovering subtle biochemical shifts in response to environmental factors like RF-EMF. More importantly, the identified metabolites may serve as candidate biomarkers for future toxicological or biosafety assessments in RF-EMF exposure studies, not only in invertebrate models but potentially in higher organisms as well.

CRediT authorship contribution statement

Yahong Wang: Writing – review & editing, Writing – original draft, Software, Project administration, Methodology, Formal analysis, Data curation. **Yanyan Liao:** Writing – review & editing, Methodology. **Peng Cai:** Writing – review & editing, Project administration. **Ziyan Zhang:** Writing – review & editing, Project administration, Formal analysis. **Lu Zhang:** Software, Investigation.

Declaration of Competing Interest

The authors declare that they have no known competing financial interests or personal relationships that could have appeared to influence the work reported in this paper.

Acknowledgements

This work is supported by the Xiamen Key Laboratory of Physical Environment. We also acknowledge the financial support from the Shanghai Military support and pension foundation.

Appendix A. Supporting information

Supplementary data associated with this article can be found in the online version at doi:10.1016/j.ecoenv.2025.119132.

Data availability

The data that has been used is confidential.

References

Altman, B.J., et al., 2016. From krebs to clinic: glutamine metabolism to cancer therapy. Nat. Rev. Cancer 16, 619–634.

Amiri, H., et al., 2023. Swimming exercise reduces oxidative stress and liver damage indices of Male rats exposed to electromagnetic radiation. Life Sci. 317, 121461.

Bektas, H., et al., 2022. Effects of 3.5 GHz radiofrequency radiation on ghrelin, nesfatin-1, and irisin level in diabetic and healthy brains. J. Chem. Neuroanat. 126.

Betta, G., et al., 2023. Human exposure to 5G systems: experimental analysis and measurement issues in FR1 and FR2 operating bands. IEEE Int. Instrum. Meas. Technol. Conf. (I2MTC 2023, 01–06.

Bouji, M., et al., 2020. Impact of cerebral radiofrequency exposures on oxidative stress and corticosterone in a rat model of alzheimer's disease. J. Alzheimers Dis. 73, 467–476.

Bredehöft, J., et al., 2019. Visualizing and profiling lipids in the OVLT of Fat-1 and wild type mouse brains during LPS-Induced systemic inflammation using AP-SMALDI MSI. ACS Chem. Neurosci. 10, 4394–4406.

Chen, L., et al., 2021. The effect of curculigo orchioides (Xianmao) on kidney energy metabolism and the related mechanism in rats based on metabolomics. Food Sci. Nutr. 9, 6194–6212.

Choi, J., et al., 2020. Continuous exposure to 1.7 GHz LTE electromagnetic fields increases intracellular reactive oxygen species to decrease human cell proliferation and induce senescence. Sci. Rep. 10, 9238.

Cordelli, E., et al., 2023. Effects of radiofrequency electromagnetic field (RF-EMF) exposure on pregnancy and birth outcomes: a systematic review of experimental studies on non-human mammals. Environ. Int. 180, 108178.

Deng, H., et al., 2024. Impact of specific electromagnetic radiation on wakefulness in mice. Proc. Natl. Acad. Sci. USA 121, e2313903121.

Di Ciaula, A., 2018. Towards 5G communication systems: are there health implications? Int J. Hyg. Environ. Health 221, 367–375.

Ding, Y., et al., 2021. Comprehensive metabolomics profiling reveals common metabolic alterations underlying the four major non-communicable diseases in treated HIV infection. eBioMedicine 71.

Eggert, T., et al., 2020. RF-EMF exposure effects on sleep - age doesn't matter in men! Environ. Res. 191.

Ehnert, S., et al., 2017. Extremely low frequency pulsed electromagnetic fields cause antioxidative defense mechanisms in human osteoblasts via induction of *O2(-) and H2O2. Sci. Rep. 7, 14544.

Gökçek-Saraç, C., et al., 2021. Possible effects of different doses of 2.1 GHz electromagnetic radiation on learning, and hippocampal levels of cholinergic biomarkers in wistar rats. Electromagn. Biol. Med. 40, 179–190.

Gorski, R., et al., 2021. Morphological and cytophysiological changes in selected lines of normal and cancer human cells under the influence of a radio-frequency electromagnetic field. Ann. Agric. Environ. Med. 28, 163–171.

Gye, M.C., Park, C.J., 2012. Effect of electromagnetic field exposure on the reproductive system. Clin. Exp. Reprod. Med. 39.

IARC, 2013. Non-ionizing radiation, part 2: radiofrequency electromagnetic fields. IARC Monogr. Eval. Carcinog. Risks Hum. 102, 1–460.

Jagbir Kaur, S.A.K., 2021. Numerical analysis of heat transfer in multilayered skin tissue exposed to 5G mobile communication frequencies. J. Therm. Eng. 7, 103–116.

Joushomme, A., et al., 2023. Effects of 5G-modulated 3.5 GHz radiofrequency field exposures on HSF1, RAS, ERK, and PML activation in live fibroblasts and keratinocytes cells. Sci. Rep. 13.

Karipidis, K., et al., 2021. 5G mobile networks and health—a state-of-the-science review of the research into low-level RF fields above 6 GHz. J. Expo. Sci. Environ. Epidemiol. 31, 585–605.

Karipidis, K., et al., 2025. The effect of exposure to radiofrequency fields on cancer risk in the general and working population: a systematic review of human observational studies - part II: less researched outcomes. Environ. Int 196, 109274.

Kesari, K.K., et al., 2011. 900-MHz microwave radiation promotes oxidation in rat brain. Electromagn. Biol. Med. 30, 219–234.

Kim, A., 2014. Mitochondrial DNA somatic mutation in cancer. Toxicol. Res 30, 235–242.

Lai, H., 2019. Exposure to static and Extremely-Low frequency electromagnetic fields and cellular free radicals. Electromagn. Biol. Med. 38, 231–248.

Lin, J.C., 2023. Incongruities in recently revised radiofrequency exposure guidelines and standards. Environ. Res 222, 115369.

Márquez, J., et al., 2017. Glutamine addiction in gliomas. Neurochem. Res. 42, 1735–1746.

Mortazavi, S.M.J., Mortazavi, S.A.R., 2016. Oxidative mechanisms of biological activity of low-intensity radiofrequency radiation. Electromagn. Biol. Med. 35, 303–304.

Mumtaz, S., et al., 2022. Microwave radiation and the brain: mechanisms, current status, and future prospects. Int. J. Mol. Sci. 23.

Nazıroğlu4, K.E.F.U.S.A.M., 2018. Long term exposure to cell phone frequencies (900 and 1800 MHz) induces apoptosis, mitochondrial oxidative stress and TRPV1 channel activation in the hippocampus and dorsal root ganglion of rats. Metab. Brain Dis. 753–763.

Neurauter, G., et al., 2008. Serum phenylalanine concentrations in patients with ovarian carcinoma correlate with concentrations of immune activation markers and of isoprostane-8. Cancer Lett. 272, 141–147.

Piccinetti, C.C., et al., 2018. Measurement of the 100 MHz EMF radiation in vivo effects on zebrafish D. Rerio embryonic development: a multidisciplinary study. Ecotoxicol. Environ. Saf. 154, 268–279.

Son, Y., et al., 2018. Long-term RF exposure on behavior and cerebral glucose metabolism in 5xFAD mice. Neurosci. Lett. 666, 64–69.

Verbeek, J., et al., 2021. Prioritizing health outcomes when assessing the effects of exposure to radiofrequency electromagnetic fields: a survey among experts. Environ. Int. 146.

Wang, Y., et al., 2022. 3.5-GHz radiofrequency electromagnetic radiation promotes the development of drosophila melanogaster. Environ. Pollut. 294, 118646.

Wang, Y.H., et al., 2021. Simulated mobile communication frequencies (3.5 GHz) emitted by a signal generator affects the sleep of drosophila melanogaster. Environ. Pollut. 283.

Wu, X.-h, et al., 2018. High-throughput metabolomics used to identify potential therapeutic targets of guizhi fuling wan against endometriosis of cold coagulation and blood stasis. RSC Adv. 8, 19238–19250.

Yang, H., et al., 2022. Effects of acute exposure to 3500 MHz (5G) radiofrequency electromagnetic radiation on Anxiety-Like behavior and the auditory cortex in Guinea pigs. Bioelectromagnetics 43, 106–118.

Yao, B.W., et al., 2025. Transcriptomic and metabolic profiling reveals the effects of long-term microwave exposure on testicular tissue. Ecotoxicol. Environ. Saf. 293.

Zubair, M., et al., 2020. Impacts of high dose 3.5 GHz cellphone radiofrequency on zebrafish embryonic development. Plos One 15.